

Identifying the Active Phenanthrene Degraders and Characterizing Their Metabolic Activities at the Single-Cell Level by the Combination of Magnetic-Nanoparticle-Mediated Isolation, Stable-Isotope Probing, and Raman-Activated Cell Sorting (MMI–SIP–RACS)

Jibing Li, Dayi Zhang, Bei Li, Chunling Luo,* and Gan Zhang



Cite This: *Environ. Sci. Technol.* 2022, 56, 2289–2299



Read Online

ACCESS |



Metrics & More



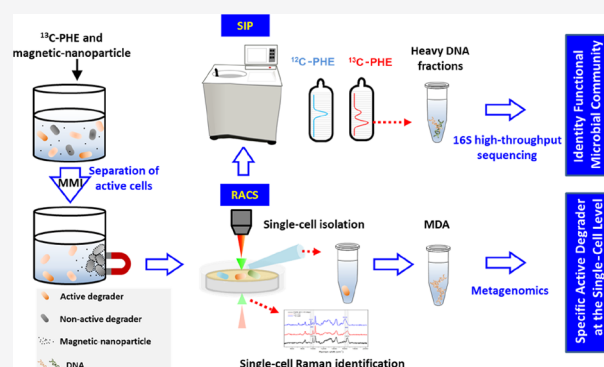
Article Recommendations



Supporting Information

ABSTRACT: Magnetic-nanoparticle-mediated isolation coupled with stable-isotope probing (MMI–SIP) is a cultivation-independent higher-resolution approach for isolating active degraders in their natural habitats. However, it addresses the community level and cannot directly link the microbial identities, phenotypes, and *in situ* functions of the active degraders at the single-cell level within complex microbial communities. Here, we used ^{13}C -labeled phenanthrene as the target and developed a new method coupling MMI–SIP and Raman-activated cell sorting (RACS), namely, MMI–SIP–RACS, to identify the active phenanthrene-degrading bacterial cells from polycyclic aromatic hydrocarbon (PAH)-contaminated wastewater. MMI–SIP–RACS significantly enriched the active phenanthrene degraders and successfully isolated the representative single cells. Amplicon sequencing analysis by SIP, ^{13}C shift of the single cell in Raman spectra, and the 16S rRNA gene from single cell sequencing *via* RACS confirmed that *Novosphingobium* was the active phenanthrene degrader. Additionally, MMI–SIP–RACS reconstructed the phenanthrene metabolic pathway and genes of *Novosphingobium*, including two novel genes encoding phenanthrene dioxygenase and naphthalene dioxygenase. Our findings suggested that MMI–SIP–RACS is a powerful method to efficiently and precisely isolate active PAH degraders from complex microbial communities and directly link their identities to functions at the single-cell level.

KEYWORDS: MMI–SIP, Raman-activated cell sorting, metagenomics analysis, *Novosphingobium*, single-cell level



1. INTRODUCTION

Petroleum hydrocarbons are ubiquitous environmental pollutants that have attracted attention worldwide because of the environmental harm that they cause.^{1,2} Polycyclic aromatic hydrocarbons (PAHs), which are toxic and carcinogenic and categorized as organic priority pollutants in environments, are considered as a major constituent of petroleum hydrocarbons.³ Biodegradation is generally considered to be a promising technique to remediate PAHs in petroleum-contaminated water.⁴ To better understand the bioremediation mechanisms of PAHs and enhance their removal efficiency ultimately, it is critical to investigate the identities and metabolic characteristics of *in situ* PAH degraders.⁵ However, this still faces a great challenge. Currently, the best way to solve this problem is to isolate PAH degraders from the environment based on the cultivation-dependent approaches and then study their metabolic characteristics to speculate on their potential roles in field remediation.^{6,7} However, these approaches highly overestimate the cultivability of microorganisms⁸ and can

hardly identify the real players, which are mostly uncultivable within a complex microbial community in their natural habitats.^{9,10}

Stable-isotope probing (SIP) is a cultivation-independent technique that can assess the metabolic responses of active degraders and link their identities to functions in the environment.¹¹ Several PAH-degrading microorganisms were successfully identified from contaminated environments using SIP.^{12–14} However, SIP usually suffers from the shift of light ^{12}C DNA into heavy ^{13}C DNA fractions, which greatly reduces the resolution and accuracy in identifying the functional microorganisms in complex microbial communities.¹⁰ Addi-

Received: July 23, 2021

Revised: January 5, 2022

Accepted: January 10, 2022

Published: January 21, 2022



tionally, SIP also cannot accurately match active microorganisms to specific phenotypes; therefore, it is often used in laboratory studies without the capability to separate the identified active degraders.

Magnetic-nanoparticle-mediated isolation (MMI) is another culture-independent technique; it can enrich and separate live active microbes from complex microbiota, enabling the investigation of their metabolic characteristics.^{15,16} However, MMI cannot accurately confirm the involvement of the enriched microorganisms in the metabolism of target pollutants or link them to specific phenotypes. In our previous work, we developed a coupled MMI–SIP method to identify active degraders in PAH-contaminated wastewater with a higher resolution and accuracy, compared with MMI or SIP alone.¹⁰ Similar to SIP, MMI–SIP can identify active degraders at the community level; it cannot link these degraders to functional genes or *in situ* genotypes at the single-cell level.^{10,14} Metagenomics, combined with SIP, can determine the genomes and metabolic functions of active microbes;^{17–19} however, it cannot accurately determine their ecological functions *in situ*. Thus, there is an urgent need to expand the current methods to explore the functional degraders of organic pollutants at the single-cell level.

Raman-activated cell sorting (RACS) is an emerging approach that can effectively isolate individual cells on the basis of their characteristics using single-cell Raman spectroscopy (SCRS).^{20,21} SCRS can reveal the intrinsic biochemical fingerprints of individual cells, such as information concerning specific biomarkers (nucleic acids, proteins, and lipids), which can help explore the physiological and metabolic profiles of active degraders at the single-cell level.^{22–24} When microbes are cultivated with a substrate labeled using stable isotopes, such as ¹³C, ¹⁵N, or ²H, certain Raman bands in the SCRS spectra shift as the active cells incorporate stable isotopes into their biomass.^{23,25,26} Therefore, SCRS combined with SIP can identify the metabolic activities of specific isotope substrates of single cells *in situ*.^{22,25,27,28} To isolate the identified single microbial cells, RACS includes a cell isolation tool in the SCRS system that sorts individual cells on the basis of their characteristics.^{22,28} Thus, RACS can achieve *in situ* detection, identification, and sorting of active degraders at the single-cell level in complex environments; it can establish a direct link between the functions and underlying genotypes of bacterial cells within complex microbial communities.^{22,25,28} RACS has been successfully used to sort carbon-fixing bacteria and antibiotic-resistant microorganisms from water and human gut microbiota,^{22,28} but it has not been used to explore the bacteria responsible for the *in situ* degradation of organic pollutants, including PAHs. Small proportions of active degraders in complex communities⁴ and poor sorting efficiency present challenges that prevent the application of RACS in the identification and sorting of the target microorganisms for ecological purposes. This provides opportunities for other strategies that may enrich the active degraders and improve the screening efficiency of RACS.

To address these challenges, we developed a novel method by coupling MMI, SIP, and RACS (MMI–SIP–RACS) to identify and isolate active PAH-degrading bacterial cells from PAH-contaminated wastewater. Because phenanthrene (PHE) is a typical model compound in the study of PAH biodegradation, we selected ¹³C-labeled PHE (¹³C-PHE) as a metabolic tracer and applied MMI–SIP–RACS to enrich (MMI), confirm (SIP), and isolate (RACS) the active PHE-

degrading microbes from a complex microbial community. In the present study, MMI successfully enriched the active PHE degraders, whose functions were subsequently confirmed by SIP; RACS further isolated the active PHE-degrading bacterial cells from their spectral shift and linked their identities to functions at the single-cell level. Our results suggest that MMI–SIP–RACS is a powerful, culture-independent method to identify and isolate active PAH degraders at the single-cell level in complex communities, with the feasibility of isolating the active degrading bacterial cells responsible for other organic pollutant mineralization in the real environment, and gives new insights into the *in situ* biodegradation mechanisms of organic pollutants.

2. MATERIALS AND METHODS

2.1. Sample Collection. The wastewater sample was collected from petroleum-contaminated industrial wastewater from the Shengli Oil Field, China (37°52'N, 118°425'E). After being transported to the laboratory in iceboxes, portions of samples were used for the initial DNA extraction and chemical analysis. The remaining samples were immediately placed at 4 °C for SIP, MMI, MMI–SIP, and MMI–SIP–RACS experiments. The physicochemical properties and PAH contents of the wastewater are listed in Table S1.

2.2. SIP, MMI, and MMI–SIP Microcosms. The microcosms were formed in 150 mL serum bottles, as described previously.¹⁰ For the SIP microcosms, unlabeled PHE (99%; Cambridge Isotope Laboratories, Inc., Tewksbury, MA, USA) or ¹³C-labeled PHE (¹³C₁₄-PHE, 99%; Cambridge Isotope Laboratories, Inc.) was added to bottles containing 50 mL of wastewater with an initial concentration of 10 mg/L. A sterile control was prepared using filter-sterilized wastewater with unlabeled PHE, while a non-PHE control was established using wastewater without PHE. Each treatment was performed in six replicates.

Before the MMI microcosm construction, biocompatible magnetic nanoparticles (MNPs) were synthesized to magnetize the microorganisms in the wastewater using the method established in our previous study.^{10,15} Microbial cell pellets were obtained by centrifuging 1.0 L of wastewater at 3000 rpm for 10 min. After resuspension in the same volume of deionized water and mixing with MNP stock solution, the mixture was shaken at 150 rpm for 20 min. The MNP-functionalized bacteria were separated from the aqueous phase using a magnet, washed three times with filter-sterilized wastewater, and finally resuspended in the filter-sterilized wastewater (1.0 L). Unlabeled PHE was then added to prepare the MMI microcosms. After 3 days of incubation, active PHE degraders were separated from inert microbes (as magnetic cell pellets) using a permanent magnet; they remained in the aqueous phase as a magnet-free cell (MFC) suspension. Portions of the MFC suspension were used for the subsequent DNA extraction. To prepare the MMI–SIP microcosms, the remaining MFCs were collected by centrifugation, transferred into the same volume of the original wastewater, split into 150 mL serum bottles (50 mL each), and supplemented with unlabeled PHE or ¹³C-PHE (final concentration 10 mg/L) using the same experimental procedures and incubation conditions as that for the SIP microcosm (Figure S1).

In total, five biotic treatments were conducted to identify and separate the active PHE degraders from the complex microbial communities: ¹²C-SIP (original wastewater with ¹²C-PHE), ¹²C-MMI–SIP (original wastewater with MFCs and

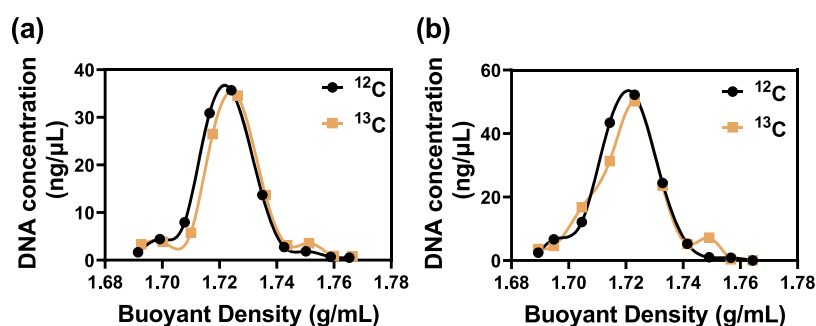


Figure 1. Correlation between the DNA concentration (ng/μL) and BD (g/mL) in DNA extracted from the SIP and MMI–SIP microcosms with ^{12}C -PHE or ^{13}C -PHE, respectively. The “light” and “heavy” DNA fractions are highlighted.

^{12}C -PHE), ^{13}C -SIP (original wastewater with ^{13}C -PHE), ^{13}C -MMI–SIP (original wastewater with MFCs and ^{13}C -PHE), and MMI (filter-sterilized wastewater with MNP-functionalized bacteria and ^{12}C -PHE). Each treatment was carried out in six replicates. After 3 and 6 days of incubation, wastewater samples from each microcosm were collected for chemical analysis. Because complete PHE degradation was observed with MMI–SIP treatment on day 6 (residual PHE = 0%, Table S2), samples were only collected on day 3 for DNA extraction to avoid cross-feeding. The details of the chemical analysis are provided in the Supporting Information.

2.3. DNA Ultracentrifugation, 16S rRNA Gene Amplicon Sequencing, and Analysis. DNA was extracted from 35 mL of each water sample from all treatments using the PowerSoil DNA isolation kit (MO BIO, Carlsbad, CA) according to the manufacturer’s instructions.⁴ Thereinto, the extracted DNA from SIP and MMI–SIP microcosms was subjected to ultracentrifugation, as previously described.¹⁰ Briefly, approximately 5 μg of DNA mixed with Tris–EDTA (pH 8.0)–CsCl solution was added to Quick-Seal polyallomer tubes (13 × 51 mm, 5.1 mL; Beckman Coulter, Pasadena, CA, USA). After balancing and sealing, the DNA in the tubes was separated using density-gradient ultracentrifugation, fractionation, and purification. The relationship between the buoyant density (BD) and DNA concentration of each fraction from SIP and MMI–SIP microcosms is illustrated in Figure 1, and the “light” and “heavy” DNA fractions were then selected to be 1.7143–1.7165 and 1.7491–1.7513 g/mL, respectively (see the Supporting Information for details).

For amplicon sequencing, the hypervariable V4 region was amplified for the DNA extracted from MFCs, as well as light DNA or heavy DNA fractions from SIP and MMI–SIP treatments using the 515f/806r primer set (BGI, Beijing, China; Table S3). Polymerase chain reaction (PCR) analysis was performed in accordance with the protocol used in our previous study.²⁹ After purification and quantification, PCR products were sequenced on an Illumina MiSeq PE250, and the sequences were subsequently analyzed in QIIME and assigned to operational taxonomic units (OTUs) at a cutoff value of 97% to generate the microbiome profiles.^{30,31}

The active PHE degraders in SIP, MMI, and MMI–SIP treatments were determined by comparing the relative enrichment factor (REF) using eqs 1 and 2, as described in previous studies.³²

$$\text{REF}_{\text{SIP or MMI-SIP}} = \left(\frac{\text{A13_heavy}}{\text{A13_light}} \right) / \left(\frac{\text{A12_heavy}}{\text{A12_light}} \right) \quad (1)$$

$$\text{REF}_{\text{MMI}} = \left(\frac{\text{A_MFC}}{\text{A_Total}} \right) \quad (2)$$

A13_heavy and A13_light are the relative abundances of OTUs in the heavy and light DNA fractions of ^{13}C -PHE (^{13}C -SIP and ^{13}C -MMI–SIP) treatments, respectively; A12_heavy and A12_light represent the relative abundances of OTUs in the heavy and light DNA fractions of ^{12}C -PHE (^{12}C -SIP and ^{12}C -MMI–SIP) treatments, respectively. For REF_{MMI} , A_MFC and A_Total refer to the relative abundances of OTUs in the MFC fractions and MMI microcosms, respectively. In the present study, OTUs with $\text{REF}_{\text{SIP or MMI-SIP}} > 1.0^{33}$ or $\text{REF}_{\text{MMI}} > 2.0^{10}$ were selected as the active PHE degraders from the top 100 OTUs, and the phylogenetic analysis of these OTUs was performed as described previously.³⁴

2.4. Spectral Acquisition and Analysis in RACS. As MMI–SIP could enrich the active PHE degraders and improve the identification accuracy, cells in ^{13}C -SIP and MFCs from ^{13}C -MMI–SIP microcosms were used for RACS, while cells in MFCs from ^{12}C -MMI–SIP microcosms were used as controls. Bacterial cells were collected by centrifugation at 5000g for 5 min and then washed twice with deionized water to remove impurities that could interfere with Raman spectral acquisition. Cell pellets were then resuspended in deionized water, spotted onto a sorting chip (1.5 μL), and air-dried at room temperature prior to the Raman spectral acquisition.²⁷ The SCRS spectra were obtained using a 532 nm Nd:YAG laser (cobolt AB, Stockholm, Sweden) with a 1200 grooves/mm diffraction grating. The Raman spectra were acquired in the range of 400–2000 cm^{-1} with 5 mW laser power and 5 s acquisition time. All measured spectra were preprocessed using Hooke IntP (HOOKE Instruments Ltd., China) for baseline correction and vector normalization.²⁸ When microbial cells assimilate the isotope-labeled substrates and synthesized macromolecules such as phenylalanine and unsaturated lipids, the heavier isotope atoms would replace the lighter atoms, changing their chemical bond vibrations and shifting their wavenumbers to lower positions.^{25,35} Based on the previous study,²⁵ the positions of Raman bands for phenylalanine and unsaturated lipids within the unlabeled cells were 1001–1003 and 1663 cm^{-1} , respectively, which shifted in the active cells incorporating ^{13}C with Raman shift extents of −37 and −35 cm^{-1} , respectively. Thus, the SCRS band positions from active degrading cells incorporating ^{13}C -PHE were determined and analyzed to establish a relationship between the red shift and ^{13}C assimilation in ^{13}C -MMI–SIP microcosms. The Raman spectra of single cells from ^{12}C -MMI–SIP samples were used as controls.

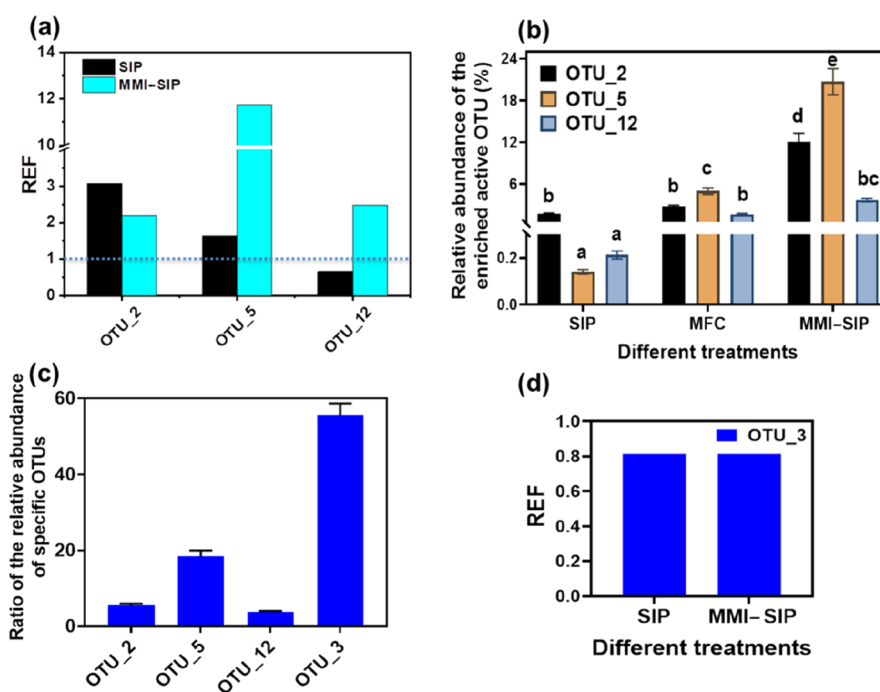


Figure 2. (a) REF of OTUs from the SIP and MMI-SIP treatments. (b) Relative abundance of the enriched OTUs in MFCs and the heavy DNA fractions of ^{13}C -SIP and ^{13}C -MMI-SIP microcosms. Data are means \pm standard deviation ($n = 3$). (c) Ratio of the relative abundance of the enriched OTUs detected in the MFCs to those in the MMI microcosms. (d) REF of OTU_3 in the SIP and MMI-SIP treatments.

2.5. Isolation of ^{13}C Cells from Wastewater by RACS and Metagenomic Sequencing. Single cells of the active PHE degraders with a ^{13}C shift were isolated using the single-cell ejection technique of RACS by PRECI SCS (HOOKE Instruments Ltd, China), as described previously.²⁸ Briefly, cells with a ^{13}C shift in the Raman spectra were sorted one by one into the collection chip containing cell lysis buffer (Qiagen) using a laser beam. The sorting process was operated by PRECI SCS software. In total, 11 individual cells were successfully isolated. They were then lysed, and the whole genomic DNA was amplified by multiple displacement amplification (MDA) using phi 29 DNA polymerase (Qiagen, Germany).²² Before sequencing using the Illumina HiSeq X-ten platform (Illumina, USA) via the PE150 strategy at Personal Biotechnology Co., Ltd. (Shanghai, China), MDA products were checked by PCR using the primer set of 27F/1492R (Table S3) to confirm the successful amplification of the sorted cells.²⁸ Two gigabytes of sequencing data were finally generated from the sorted single cells and filtered to remove short reads with the nucleotides (nt) < 80 and the mean quality score of < 25. To remove human contamination, the reads were mapped against the human reference genome (build 37) with a Blastn E -value threshold of $\leq 10^{-5}$, a bitscore of ≥ 50 , and a percentage identity of $\geq 75\%$ through bowtie2 (version 2.1.0).³⁶ Short sequence data were assembled into high-quality contigs with a MEGAHIT assembler.³⁷ In total, 561 assembled contigs with the length > 1000 bp were obtained and used for protein sequence prediction and annotation by Prokka version 1.12.³⁸ The metagenome was assembled and obtained through multiple binning tools such as MaxBin2 and metaBAT2 in MetaWRAP,³⁹ and its completion and contamination were evaluated by checkM software.³⁸ To identify the KEGG metabolic pathways, clean short sequences aligned to the UniRef90 database were inferred using HUMAnN2 software.⁴⁰ Because the KEGG database only

contains *nahAc* and *nidA* genes from particular microbes (e.g., *Pseudomonas* and *Mycobacterium*), GhostKOALA could not recognize the genes involved in the first steps of PHE degradation from the identified degraders, particularly, the dominant lineages including *Sulfuritalea* and *Novosphingobium*. Therefore, to avoid missing PAH degradation-related metabolic pathways and genes in KEGG, we also used the AromaDeg database to detect the functional genes potentially involved in the aerobic degradation of aromatic compounds with the following alignment parameters: E value > 0.00001, identity > 50%, query coverage > 50%, and subject coverage > 30%.⁴¹ The sequences related to AromaDeg enzyme families were subsequently aligned using MAFFT with an L-INS-i strategy⁴² and edited using JalView 2.⁴³ The phylogenetic information regarding these alignments was analyzed using a previously described method.⁴⁴ All sequence data were deposited in the NCBI public database with the BioProject accession PRJNA741712.

2.6. Chemical Analysis. PHE in wastewater from each sample (days 0, 3m and 6) was analyzed using gas chromatography mass spectrometry (GC-MS) (Agilent 7890) as previously described.²⁹ Briefly, water samples were spiked with 1000 ng of deuterated PAHs and extracted twice with dichloromethane. After concentration and purification using a silica-gel/alumina column (8 mm i.d.), the eluent was concentrated to approximately 0.5 mL with N_2 . Before the instrumental analysis, 1000 ng of hexamethylbenzene was added as an internal standard. The concentrations of deuterated PAHs, PAH standards, and the internal standard are listed in Table S4.

2.7. Statistical Analysis. All experiments were performed independently in at least biological triplicate. Data were analyzed by ANOVA and independent-sample t -test methods.⁴⁵ Figures were plotted using R and Origin 8.0.^{12,46} The phylogenetic information concerning active degraders was

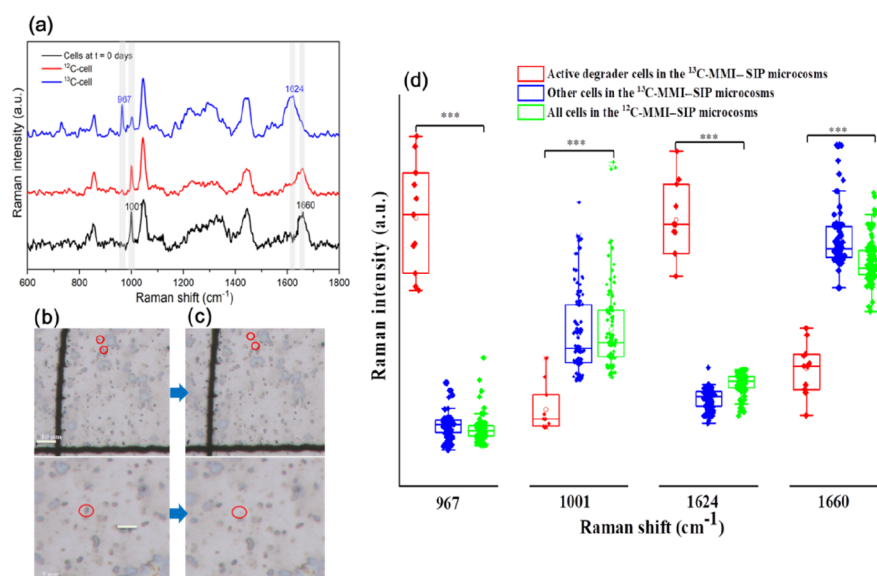


Figure 3. RACS of the active PHE degraders in wastewater. (a) SCRS spectra of cells after *in situ* culturing with unlabeled PHE and ¹³C-PHE in MMI-SIP microcosms, tagged as ¹²C-cell and ¹³C-cell, respectively. Cells at *t* = 0 days mean Raman spectra of cells treated with ¹³C-PHE at time *t* = 0 days. Each spectrum represents an average of SCRS from 11 single cells. (b) Cells of the active PHE degraders on the sorting chip were identified by SCRS from the ¹³C-MMI-SIP microcosms. (c) Cells were ejected off the sorting chip by RACS. (d) Intensity of Raman bands at 967, 1001, 1624, and 1660 cm⁻¹ from the active cells detected in ¹³C-MMI-SIP, other cells in the ¹³C-MMI-SIP microcosms, as well as cells in the ¹²C-MMI-SIP. All comparisons denoted by asterisks (***) and a black bar are significantly different (one-way ANOVA, *P* < 0.001).

determined using BLAST (National Center for Biotechnology Information, USA). *p* values < 0.05 and <0.001 were considered statistically significant and highly significant, respectively; statistical analyses were carried out using SPSS software (ver. 24.0; SPSS Inc., USA). Data are expressed as means ± standard deviations.

3. RESULTS

3.1. PHE Degradation Performance and Microbial Community Change. PHE recovery rates during the extraction procedure were 77–84% in this study. All biotic treatments (¹²C-SIP, MMI, and ¹²C-MMI-SIP microcosms) showed significant PHE elimination (Table S2), whereas more than 86.7% of the PHE remained in the sterile controls (CK); this confirmed the occurrence of PHE biodegradation. On day 3, residual PHE percentage is 38.4% and 37.7% in the SIP and MMI microcosms, respectively; these values were significantly higher than that in MMI-SIP microcosms (16.3%; *p* < 0.05). This finding suggested that MFCs separated from MMI microcosms contributed 21.4–22.1% of the PHE degradation in wastewater. Our results indicated that bioaugmentation using MFCs separated from indigenous microbiota *via* MMI could significantly enhance the PHE biodegradation in industrial wastewater.

The dominant bacteria in the original wastewater included members of the genera *Aquabacterium* (83.5%), *Zavarzinia* (6.04%), and *Comamonas* (5.72%) (Figure S2). However, the microbial community structure significantly changed in the SIP, MFC, and MMI-SIP microcosms after 3 days of incubation. Compared with that in the original wastewater, the relative abundances of *Aquabacterium* and *Zavarzinia* significantly declined in the SIP and MFC treatments, while *Pseudomonas* (4.58%) and *Azospirillum* (4.33%) became the dominant microbes in the SIP microcosms and *Novosphingobium* (5.83%) and *Methyloversatilis* (32.2%) became the dominant microbes in the MFC treatment. Moreover, the

addition of MFC suspension to wastewater induced a significant change in the microbial composition in the MMI-SIP microcosms, compared with that in the SIP microcosms. In particular, *Novosphingobium* was significantly more abundant in the MMI-SIP microcosms (10.9%) than that in the SIP microcosms (0.45%, *p* < 0.05).

3.2. Active PHE Degraders as Revealed by SIP, MMI, and MMI-SIP. Based on the correlations between the DNA concentration and BD values (Figure 1), DNA in the fractions with BDs of 1.71651 and 1.75018 g/mL was selected as the “light” and “heavy” DNA fractions for the SIP microcosms, respectively. The active degraders responsible for ¹³C-PHE assimilation were determined by the REF values of the top 100 OTUs based on their relative abundance. As shown in Figure 2a, the REF values of OTU_2 and OTU_5 were 3.07 and 1.64, respectively, indicating their critical roles in *in situ* PHE degradation. Figure S3 shows the phylogenetic information of these active PHE degraders in the SIP microcosms. OTU_2 belongs to genus *Sulfuritalea* of *Sterolibacteriaceae* (phylum Proteobacteria, class Betaproteobacteria, and order Nitrosomonadales). OTU_5 is assigned to genus *Novosphingobium* of *Sphingomonadaceae* (phylum Proteobacteria, class Alphaproteobacteria, and order Sphingomonadales) and shares 99.6% similarity with *Novosphingobium* sp. strain N25 (MK757924.1) and *Novosphingobium aromaticivorans* strain KIT-006 (MK886596.1).

In the MMI microcosms (Figure 2c), four OTUs were enriched in the MFCs, including OTU_2, OTU_5, OTU_12, and OTU_3 with REF values of 5.49, 18.4, 3.78, and 55.5, respectively. Among them, microorganisms represented by OTU_2 and OTU_5 were identified as the active PHE degraders in the SIP microcosms, and MMI results further confirmed their critical roles in the *in situ* PHE mineralization. However, OTU_12 and OTU_3 were not detected as the PHE degraders according to the SIP results, and thus, their PHE degradation capability was questioned (Figure 2a,d). It is

noteworthy that the relative abundance of *Novosphingobium* represented by OTU_5 in the MFCs (5.83%) of the MMI microcosms was more than 11.9 times higher than that in the SIP microcosms (0.45%), hinting the significant enrichment of the active PHE degraders by MMI (Figure S3). In the MMI-SIP microcosms, three OTUs, including two OTUs determined in the SIP microcosms and one OTU characterized in the MMI treatments, were identified as PHE degraders since the REF values of these OTUs were 2.21 (OTU_2), 11.8 (OTU_5), and 2.47 (OTU_12) respectively (Figure 2a). Obviously, the REF values of OTU_5 and OTU_12 significantly increased in the MMI-SIP microcosms compared with the SIP results, indicating a higher resolution of MMI-SIP to identify the active degraders. The relative abundance of OTU_5 in the heavy DNA fractions of the ^{13}C -MMI-SIP microcosms was 20.7%, approximately 146-fold higher than that in the SIP treatments (0.14%), and the REF value increased by 6.19-fold, compared with that in the SIP microcosms. This result indicated a remarkable enrichment of the microbes, represented by OTU_5 in the MMI-SIP microcosms as the most active degraders within the PHE-degrading microbial community (Figure 2b). Additionally, the relative abundance of OTU_5 in the ^{13}C -MMI-SIP treatments (10.9%) was >23 times higher than that in the SIP microcosms (0.45%), further confirming the significant enrichment of active PHE degraders by MMI-SIP (Figure S4). For OTU_12, which was not incorporated with ^{13}C -PHE assimilation in the SIP microcosms, its representative microbes performed the PHE degradation capacity in the MMI-SIP treatments. Based on the phylogenetic tree of active PHE degraders (Figure S3), OTU_12 belongs to genus *Blastomonas* of *Sphingomonadaceae* (phylum Proteobacteria, class Alphaproteobacteria, and order Sphingomonadales) and shares 99.1% similarity with *Blastomonas* sp. TW1 (AY704922.1) and *Blastomonas* sp. CF7 (AY704921.1).

Overall, SIP could accurately identify the active PHE degraders, but their abundance was too low for the subsequent RACS. MMI significantly enriched the active degraders but failed in confirming their actual functions as compared with SIP results. The combination of these two approaches (MMI-SIP) confirmed the PHE degradation functions of the identified microbes and successfully enriched them within the whole microbiota, which was conducive to the subsequent isolation of active degrading cells by RACS.

3.3. In Situ Identification and Isolation of the Active PHE-Degrading Cells Exhibiting a ^{13}C Shift in the SCRS Spectra. MMI-SIP-RACS was used to isolate the active PHE degraders in the wastewater microbial community based on the significant shifts of Raman bands caused by ^{13}C incorporation in microbial cells by SCRS.²⁵ Figure 3a illustrates the significant band shifts of some cells in the ^{13}C -MMI-SIP microcosms compared to that of the ^{12}C -MMI-SIP microcosms. Cells from the ^{12}C -MMI-SIP microcosms exhibited two identical Raman bands at 1001 and 1660 cm^{-1} as biomarkers for unlabeled cells. They were associated with the symmetric ring breathing mode of phenylalanine and C=C of unsaturated lipids, respectively.²⁵ In the ^{13}C -MMI-SIP microcosms, some cells exhibited remarkable red shifts from 1001 to 967 cm^{-1} and from 1660 to 1624 cm^{-1} (Raman shift extents of 34 and 36 cm^{-1} , respectively), consistent with the findings in previous studies.^{25,47} Therefore, these cells were the active PHE degraders incorporating ^{13}C -PHE.

For the ^{13}C -SIP, ^{12}C -MMI-SIP, and ^{13}C -MMI-SIP microcosms, 400, 400, and 1200 cells were detected by SCRS, respectively. No bacterial cells with a ^{13}C shift from 1001 to 967 or from 1660 to 1624 cm^{-1} were observed in the ^{13}C -SIP and ^{12}C -MMI-SIP treatments. In the ^{13}C -MMI-SIP microcosms, 11 single cells (approximately 1% of all detected cells) exhibited identical ^{13}C -shifted bands and were sorted using RACS (Figure 3b,c). Raman intensities of the bands at 967, 1001, 1624, and 1660 cm^{-1} (Figure 3d) illustrated no significant differences between the cells in the ^{12}C -MMI-SIP microcosms and nonactive cells in the ^{13}C -MMI-SIP microcosms ($p > 0.05$). The active PHE-degrading cells in the ^{13}C -MMI-SIP microcosms exhibited remarkably higher intensities at 967 and 1624 cm^{-1} but lower intensities at 1001 and 1660 cm^{-1} ($p < 0.001$). This result confirmed that MMI-SIP-RACS could effectively identify the active PHE-degrading cells. Importantly, RACS failed in directly sorting the active PHE degraders in ^{13}C -SIP microcosms, explained by their extremely low abundance (<1% from SIP results). Thus, MMI-SIP-RACS greatly enriched the active degraders from the whole community and benefited the sorting efficiency by RACS.

Considering the challenge to amplify an individual cell and obtain enough genetic information, all the sorted cells processed for MDA were combined and subjected to sequencing. A sequence without any double peak was obtained, indicating that the sorted cells were nearly identical. The length of the 16S rRNA gene sequence was 1402 bp after multiple alignments, and high 16S rRNA gene sequence similarities were found between the sorted cells and OTU_5 (100%), *Novosphingobium* sp. strain N25 (99.4%), or *N. aromaticivorans* strain KIT-006 (99.1%) (Figure S5). This result indicated that the sorted cells were the active PHE degrader *Novosphingobium*, represented by OTU_5. The metagenomics functional profile (MFP) analysis revealed a relative abundance of microbial population associated with *Novosphingobium* (99.7%) (Table S5), confirming the identity of the sorted cells. In addition, one assembled bin (bin 1) with a high completeness of 83.1% was generated from the sorted cells assimilating ^{13}C . Although 16S rRNA genes were not detected in the metagenome-assembled genomes, another molecular taxonomic marker (the *gyrB* gene) was identified, and its phylogenetic tree showed that bin 1 was most closely related to *N. aromaticivorans* (WP_011446947.1) and *N. aromaticivorans* (SCY28706.1) with a high similarity of 100% and formed a subclade with a high bootstrap value of 100 (Figure S6).

3.6. Linking the Genotypes and Functions of Active PHE Degraders and Reconstruction of the PHE Metabolic Pathway. Based on the KEGG database analysis, the metabolic profiles of the sorted PHE degraders were explored and linked to the genotypes. We detected 22 functional categories; the metabolisms of carbohydrates (15.6%), cofactors and vitamins (12.8%), amino acids (12.6%), lipids (10.1%), terpenoids and polyketides (8.02%), and xenobiotics (6.94%) had high relative abundances (>6%) (Figure S7a). In the carbohydrate metabolisms with the highest relative abundances, genes associated with 13 functional categories (e.g., metabolisms of butanoate, pyruvate, propanoate, glyoxylate, and dicarboxylate) were detected, suggesting that the sorted cells could use these substances as carbon sources (Figure S7b). In addition, some genes were involved in the metabolism of cofactors and vitamins, including

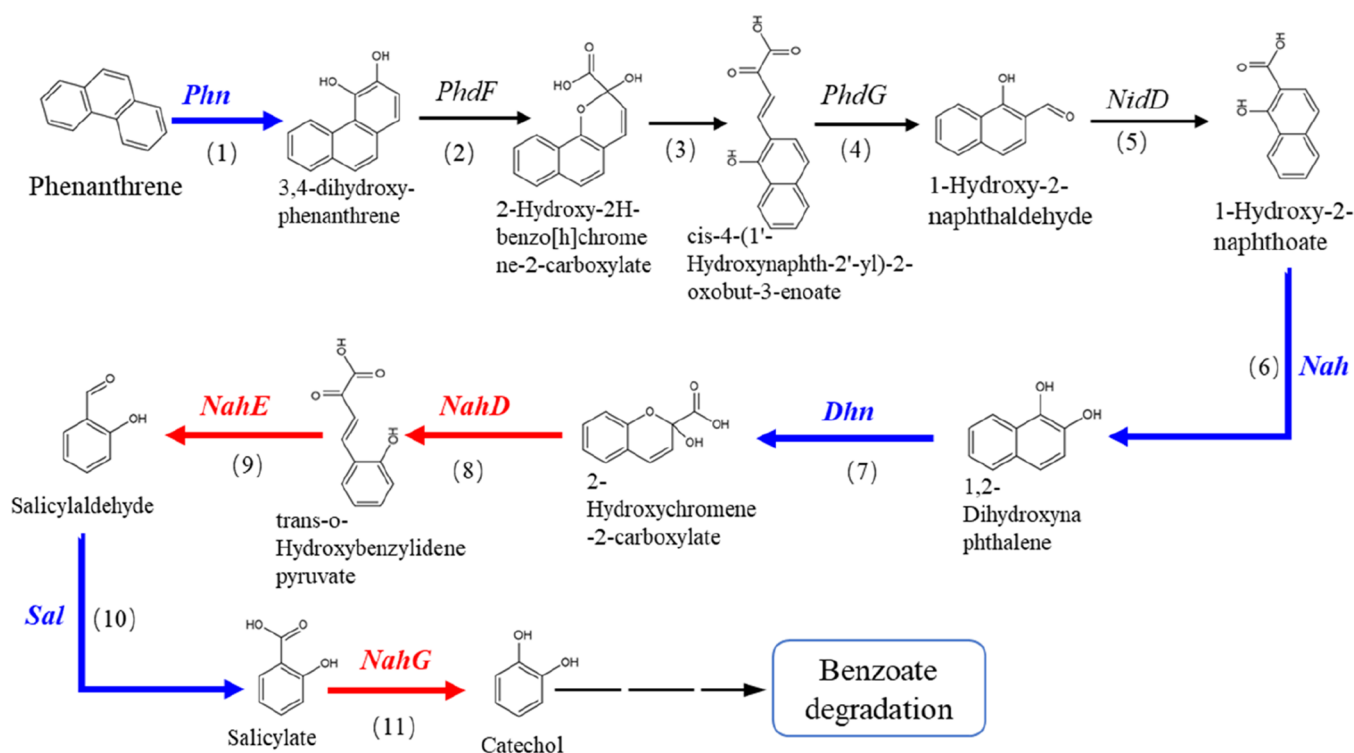


Figure 4. Reconstruction of the PHE metabolic pathway of the sorted cells incorporating ^{13}C -PHE characterized by RACS. Blue arrows represent genes described in AromaDeg. Red arrows are genes found in GhostKOALA. The genes of *PhdF*, *PhdG*, and *NidD* were not detected in the both GhostKOALA annotation and AromaDeg database. The numbers stand for the enzymes as follows: (1) PHE dioxygenase (*Phn*), (2) extradiol dioxygenase (*PhdF*), (3) epimerase, (4) hydratase–aldolase (*PhdG*), (5) aldehyde dehydrogenase (*NidD*), (6) naphthalene dioxygenase (*Nah*), (7) 1,2-dihydroxynaphthalene dioxygenase (*Dhn*), (8) 2-hydroxychromene-2-carboxylate isomerase (*NahD*), (9) *trans*-o-hydroxybenzylidenepyruvate hydratase-aldolase (*NahE*), (10) salicylaldehyde dehydrogenase (*Sal*), and (11) salicylate hydroxylase (*NahG*).

vitamins B1, B2, B3, B6, B7, B9, and lipoic acid; these are important substances for the growth and cultivation of microorganisms (Figure S7c).⁴⁸ Although we identified some functional categories related to the xenobiotic biodegradation and metabolism, which involved the biodegradation of aromatic compounds (e.g., aminobenzoate, benzoate, bisphenol, and chlorobenzene), the subcategories of PAH degradation were not detected in the sorted PHE-degrading bacterial cells (Figure S7d). However, based on the GhostKOALA annotation results, functional genes [e.g., encoding 2-hydroxychromene-2-carboxylate isomerase (*NahD*), *trans*-o-hydroxybenzylidenepyruvate hydratase-aldolase (*NahE*), and salicylate hydroxylase (*NahG*)] involved in the naphthalene/salicylate pathway of PHE degradation were detected, while other functional genes of the pathway were not found (Figure 4). Furthermore, according to the AromaDeg database, functional genes related to PHE dioxygenase (*Phn*), naphthalene dioxygenase (*Nah*), 1,2-dihydroxynaphthalene dioxygenase (*Dhn*), and salicylaldehyde dehydrogenase (*Sal*) were identified. Combining the findings from analyses using these two databases, we directly linked the functions of the active PHE degrader *Novosphingobium* to their genotypes; we successfully mapped a reasonably complete naphthalene/salicylate pathway of the PHE metabolism for the sorted cells (Figure 4). Among the detected functional genes, two novel genes, *Phn* and *Nah*, had 56.4% and 65% similarities with the *Phn* gene in *Acidovorax* sp NA3 (ACG70971) and the *Nah* gene in *Pseudomonas* sp ND6 (NP_943188), respectively (Table S6).

4. DISCUSSION

SIP, MMI, and RACS are three cultivation-independent approaches for the identification of active microbes with specific functions in their natural habitats.^{10,11} SIP relies on the incorporation of a stable isotope-labeled substrate; it identifies active degraders by analyzing the isotope-enriched cellular components at a microbial community level.⁶ Thus, SIP is a powerful technique that establishes a precise link between the microbe and its functions in the environment.⁴¹ MMI is a recently developed approach that separates and enriches live active degraders from complex microbial communities using magnets, without any need for substrate labeling.^{10,15} This technique is conducive to other follow-up studies of active microbes, such as physiological and metabolic analyses.¹⁵ RACS is a powerful tool that identifies and isolates bacterial cells on the basis of their Raman spectra, providing clues for active (particularly uncultured) microorganisms in the natural environment at the single-cell level.²⁸ SCRS is label-free method that can characterize chemical changes within single cells; it can distinguish physiological states and metabolic activities.^{22,27} Combined with SIP, RACS could sort active bacterial cells on the basis of their phenotypic characteristics, directly linking them to functions and genotypes.^{22,28}

In the present study, SIP successfully identified *Sulfuritalea*, represented by OTU_2 (1.72% of the total population), and *Novosphingobium*, represented by OTU_5 (0.14% of the total population), as the active PHE degraders responsible for the *in situ* PHE metabolism. SIP has been reported to accurately identify active but yet-to-be-cultivated microorganisms in the environment, revealing their *in situ* ecological functions at the

microbial community level.^{6,10} However, the use of this approach to link active degraders and their functional genes, or to establish a link between phenotypes and genotypes within complex microbial communities, is challenging.²⁵ Additionally, SIP as a molecular tool cannot unravel the physicochemical and metabolic properties of active degraders or improve their efficiencies in mineralizing the pollutants; the identified degraders cannot be used for practical applications. Furthermore, SIP only obtains a small amount of DNA, and genome acquisition may be challenging.

Four OTUs, including two SIP-identified PHE degraders (OTU_2 and OTU_5), were enriched in MMI (Figure 2a,d). Moreover, MMI significantly increased the abundances of these two OTUs in MFCs. However, OTU_12 and OTU_3 were not identified as active PHE degraders in SIP, which makes their role in the PHE metabolism unclear. Thus, MMI alone could not accurately confirm the active degraders and determine their functions¹⁰ because other fast-growing bacteria could also be enriched.^{10,15} Despite its lower accuracy than that of SIP, MMI has the unique advantage that it can effectively separate and enrich live active microbes from the microbial community,¹⁶ particularly, *Novosphingobium*, which enhanced the sorting efficiency of active degrading cells in RACS in this study. Additionally, bioaugmentation using these separated microbes significantly enhanced the PHE biodegradation in wastewater by 21.4–22.1% ($p < 0.05$), which was >10% better than our previous findings.²⁹ This suggests considerable potential for the MMI-enriched degrading microflora to improve the remediation of environmental pollutants.

Single-cell analysis is increasingly important for the isolation of bacterial cells and characterization of their metabolic activities within complex microbial communities.^{25,49} RACS is a recently developed method that can sort active bacterial cells based on their characteristic peak in the SCRS spectra.^{23,28} As a nondestructive and noninstructive approach, RACS has been widely applied to identify targeted cells and determine their phenotypic characteristics.^{25,26,49} Additionally, the combination of RACS and SIP can identify the metabolic activities of isotope-labeled substrates of single cells *in situ*.^{25,26,50} SIP–RACS has been used successfully to explore the metabolic functions of various microbes (e.g., N_2 -fixing bacteria,²⁷ carbon-fixing bacteria,²² and antibiotic-resistant microorganisms²⁸) at the single-cell level within complex communities. However, it has not yet been applied in the field of organic pollutant degradation. The small proportion of functional microbes in the microbiota makes it challenging to use RACS for detecting and isolating the active microorganisms. In this study, we developed an MMI–SIP–RACS approach to identify, enrich, and confirm the genotypes and phenotypes of active PHE degraders at the single-cell level. The active degrader, *Novosphingobium*, was accurately identified within the complex microbial community by SIP, enriched and separated by MMI, and eventually isolated from ¹³C–MMI–SIP microcosms by RACS using the SCRS ¹³C shift. In contrast to ¹³C–SIP microcosms, which failed to sort the active degraders (0 of 400 cells), MMI–SIP–RACS achieved a significantly improved sorting efficiency (11 of 1200 cells). Two biomarkers of the symmetric ring breathing mode of phenylalanine (1001 cm^{-1}) and C=C of unsaturated lipids (1660 cm^{-1}) were effective for confirming the incorporation of ¹³C from ¹³C–PHE into the active degraders (Figure 3). These two vibrational bands have previously been used as fingerprint

biomarkers to identify the microcosms incorporated with ¹³C-labeled compounds, such as ¹³C-glucose and ¹³C-phenylalanine.^{25,47,51} Accordingly, our MMI–SIP–RACS approach overcomes the limitations of each technology; it efficiently identifies the active PHE degraders, linking their identities and functions at the single-cell level.

Novosphingobium, sorted by MMI–SIP–RACS, belongs to the *Sphingomonadaceae* family of *Alphaproteobacteria*; it constitutes a Gram-stain-negative, aerobic, rod-shaped bacterium. Members of this genus are found in a wide range of ecological habitats, such as deep-sea water,⁵² freshwater sediments,⁵³ and oil-polluted soils.⁵⁴ They exhibit versatile metabolic capabilities of degrading several aromatic hydrocarbons,^{53,55} including 1-methylnaphthalene,⁵⁴ PHE, and naphthalene.^{4,48,56} However, the link between *Novosphingobium* and PHE degradation was not confirmed by RACS at the single-cell level prior to this study. Furthermore, the genes associated with the PHE metabolism in *Novosphingobium* were characterized by RACS after MDA and metagenomic sequencing, which further confirmed its role. Two novel PHE-degradation genes (*Phn* and *Nah*) were detected in the sorted *Novosphingobium* cells, which were not previously assigned to this genus. These genes might have been shared among genera through some evolutionary processes, such as horizontal gene transfer. Microbes usually obtain heterogenous genes from other microorganisms through horizontal gene transfer to adapt to difficult environmental conditions.⁵⁷ Our results provided evidence that the horizontal transfer of PHE degradation-related genes may occur in wastewater. Additionally, MMI–SIP–RACS successfully reconstructed the PHE degradation pathway for the sorted *Novosphingobium*, suggesting that the approach could help obtain new degradation-related genes and identify new degradation mechanisms. Surprisingly, we did not obtain any cells of the other two MMI–SIP identified active degraders, *Sulfuritalea* (OTU_2) and *Blastomonas* (OTU_12), possibly explained by their low abundances in the ¹³C–MMI–SIP microcosms (0.18 and 1.17%, respectively). They are usually associated with the benzoate of aesculin degradation,^{58,59} but they have not yet been linked to PHE degradation. Our MMI–SIP results provided unequivocal evidence that members of these two genera were directly involved in the PHE degradation in petroleum-contaminated wastewater.

Overall, MMI–SIP–RACS is a powerful cultivation-independent approach that can accurately and efficiently isolate single cells of active PHE degraders from complex wastewater microbial communities, particularly functional-yet-uncultivable microbes with low abundances. This novel technique combines the advantages of MMI, SIP, and RACS to complement each other, thus offering opportunities to directly link the microbes to phenotypes and explore the mechanisms of PAH metabolism. It is also feasible for the identification, separation, and application of active degrading bacteria for other organic pollutants, facilitating the acquisition of new insights into their degradation mechanisms..

■ ASSOCIATED CONTENT

Supporting Information

The Supporting Information is available free of charge at <https://pubs.acs.org/doi/10.1021/acs.est.1c04952>.

Concentrations of PAHs in wastewater; residual PHE percentage in wastewater; primers used for the PCR of

the 16S rRNA gene; components of deuterated PAHs, standards, and the internal standard; MFP of the sorted cells by RACS; functional genes of the sorted cells incorporating ^{13}C from ^{13}C -PHE characterized by RACS; schematic protocols of separating and identifying the functional microbes from the whole microbiota via MMI-SIP-RACS, compared to those via SIP, MMI, and MMI-SIP alone; relative abundance of 16S rRNA-defined taxa at genus level in SIP, MFC, and MMI-SIP microcosms; phylogenetic tree of the identified OTUs responsible for the in situ PHE degradation, with the neighbour-joining tree based on 16S rRNA gene sequences showing the phylogenetic position of the microorganisms corresponding to OTU_2, OTU_5, and OTU_12 and their representatives of some other related taxa; whole community structure in the ^{13}C -SIP, MFC, and ^{13}C -MMI-SIP microcosms after 3 day incubation; phylogenetic tree of the sorted target cells responsible for the in situ PHE degradation, with the neighbour-joining tree based on 16S rRNA gene sequences showing the phylogenetic position of the sorted PHE-degrading bacterial cells and its representatives of some other related taxa; phylogenetic tree of the assembled bin of the sorted PHE-degrading cells assimilating ^{13}C identified by RACS results based on the neighbour-joining method using *gyrB* gene sequences, showing the phylogenetic position of the bacterium associated with the active PHE degraders and representatives of some related taxa; functional analysis of shotgun metagenomic aligned sequences from sorted cells incorporating ^{13}C from ^{13}C -PHE characterized by RACS based on the KEGG pathway database; and relative abundance of 22 functional categories, 13 carbohydrate metabolism categories, 6 functional categories associated with the metabolism of cofactors and vitamins, and 5 functional categories related to the xenobiotics biodegradation and metabolism (PDF)

AUTHOR INFORMATION

Corresponding Author

Chunling Luo – State Key Laboratory of Organic Geochemistry and Guangdong Provincial Key Laboratory of Environmental Protection and Resources Utilization, Guangzhou Institute of Geochemistry, Chinese Academy of Sciences, Guangzhou 510640, China; CAS Center for Excellence in Deep Earth Science, Guangzhou 510640, China; University of Chinese Academy of Sciences, Beijing 100039, China; orcid.org/0000-0003-2359-4246; Phone: +86-20-85290290; Email: cluo@gig.ac.cn; Fax: +86-20-85290706

Authors

Jibing Li – State Key Laboratory of Organic Geochemistry and Guangdong Provincial Key Laboratory of Environmental Protection and Resources Utilization, Guangzhou Institute of Geochemistry, Chinese Academy of Sciences, Guangzhou 510640, China; CAS Center for Excellence in Deep Earth Science, Guangzhou 510640, China; University of Chinese Academy of Sciences, Beijing 100039, China; orcid.org/0000-0003-3115-9017

Dayi Zhang – College of New Energy and Environment, Jilin University, Changchun 130021, China

Bei Li – The State Key Lab of Applied Optics, Changchun Institute of Optics, Fine Mechanics and Physics, Chinese Academy of Sciences, 130033 Changchun, China; HOOKE Instruments Ltd., 130033 Changchun, China

Gan Zhang – State Key Laboratory of Organic Geochemistry and Guangdong Provincial Key Laboratory of Environmental Protection and Resources Utilization, Guangzhou Institute of Geochemistry, Chinese Academy of Sciences, Guangzhou 510640, China; CAS Center for Excellence in Deep Earth Science, Guangzhou 510640, China; orcid.org/0000-0002-9010-8140

Complete contact information is available at:

<https://pubs.acs.org/10.1021/acs.est.1c04952>

Author Contributions

C.L., J.L., and D.Z. designed the experiments; J.L. performed the experiments; J.L. and B.L. collected and analyzed the data; J.L. wrote the first draft of the manuscript; and J.L., C.L., D.Z., and G.Z. revised the manuscript.

Notes

The authors declare no competing financial interest.

ACKNOWLEDGMENTS

Financial support was provided by the Key-Area Research and Development Program of Guangdong Province (2020B1111530003), the National Natural Science Foundation of China (nos. 32061133003 and 41907298), the Natural Science Foundation of Guangdong Province, China (2021A1515011561), and the Guangdong Foundation for Program of Science and Technology Research (no. 2020B1212060053). This paper was also granted the Tuguangchi Award for Excellent Young Scholar GIGCAS and the State Key Laboratory of Organic Geochemistry, GIGCAS (grant no. SKLOG2020-8).

REFERENCES

- (1) Barron, M. G.; Vivian, D. N.; Heintz, R. A.; Yim, U. H. Long-Term Ecological Impacts from Oil Spills: Comparison of Exxon Valdez, Hebei Spirit, and Deepwater Horizon. *Environ. Sci. Technol.* **2020**, *54*, 6456–6467.
- (2) Tran, H.-T.; Lin, C.; Bui, X.-T.; Ngo, H.-H.; Cheruiyot, N. K.; Hoang, H.-G.; Vu, C.-T. Aerobic composting remediation of petroleum hydrocarbon-contaminated soil. Current and future perspectives. *Sci. Total Environ.* **2021**, *753*, 142250.
- (3) Fernando, H.; Ju, H.; Kakumanu, R.; Bhople, K. K.; Croissant, S.; Elferink, C.; Kaphalia, B. S.; Ansari, G. A. S. Distribution of petrogenic polycyclic aromatic hydrocarbons (PAHs) in seafood following Deepwater Horizon oil spill. *Mar. Pollut. Bull.* **2019**, *145*, 200–207.
- (4) Li, J.; Luo, C.; Song, M.; Dai, Q.; Jiang, L.; Zhang, D.; Zhang, G. Biodegradation of Phenanthrene in Polycyclic Aromatic Hydrocarbon-Contaminated Wastewater Revealed by Coupling Cultivation-Dependent and -Independent Approaches. *Environ. Sci. Technol.* **2017**, *51*, 3391–3401.
- (5) Dombrowski, N.; Donaho, J. A.; Gutierrez, T.; Seitz, K. W.; Teske, A. P.; Baker, B. J. Reconstructing metabolic pathways of hydrocarbon-degrading bacteria from the Deepwater Horizon oil spill. *Nat. Microbiol.* **2016**, *1*, 16057.
- (6) Dumont, M. G.; Murrell, J. C. Stable isotope probing - linking microbial identity to function. *Nat. Rev. Microbiol.* **2005**, *3*, 499–504.
- (7) Ping, L.; Guo, Q.; Chen, X.; Yuan, X.; Zhang, C.; Zhao, H. Biodegradation of pyrene and benzo[a]pyrene in the liquid matrix and soil by a newly identified *Raoultella planticola* strain. *3 Biotech* **2017**, *7*, 56.

- (8) Rappé, M. S.; Giovannoni, S. J. The Uncultured Microbial Majority. *Annu. Rev. Microbiol.* **2003**, *57*, 369–394.
- (9) Amann, R. I.; Ludwig, W.; Schleifer, K. H. Phylogenetic identification and in situ detection of individual microbial cells without cultivation. *Microbiol. Rev.* **1995**, *59*, 143–169.
- (10) Li, J.; Luo, C.; Zhang, G.; Zhang, D. Coupling magnetic-nanoparticle mediated isolation (MMI) and stable isotope probing (SIP) for identifying and isolating the active microbes involved in phenanthrene degradation in wastewater with higher resolution and accuracy. *Water Res.* **2018**, *144*, 226–234.
- (11) Neufeld, J. D.; Vohra, J.; Dumont, M. G.; Lueders, T.; Manefield, M.; Friedrich, M. W.; Murrell, J. C. DNA stable-isotope probing. *Nat. Protoc.* **2007**, *2*, 860–866.
- (12) Li, J.; Luo, C.; Zhang, D.; Cai, X.; Jiang, L.; Zhang, G. Stable-isotope probing enabled cultivation of the indigenous strain *Ralstonia* sp. M1 capable of degrading phenanthrene and biphenyl in industrial wastewater. *Appl. Environ. Microbiol.* **2019**, *85*, No. e00511-19.
- (13) Li, J.; Luo, C.; Zhang, D.; Cai, X.; Jiang, L.; Zhao, X.; Zhang, G. Diversity of the active phenanthrene degraders in PAH-polluted soil is shaped by ryegrass rhizosphere and root exudates. *Soil Biol. Biochem.* **2019**, *128*, 100–110.
- (14) Li, J.; Zhang, D.; Song, M.; Jiang, L.; Wang, Y.; Luo, C.; Zhang, G. Novel bacteria capable of degrading phenanthrene in activated sludge revealed by stable-isotope probing coupled with high-throughput sequencing. *Biodegradation* **2017**, *28*, 423–436.
- (15) Zhang, D.; Berry, J. P.; Zhu, D.; Wang, Y.; Chen, Y.; Jiang, B.; Huang, S.; Langford, H.; Li, G.; Davison, P. A.; Xu, J.; Aries, E.; Huang, W. E. Magnetic nanoparticle-mediated isolation of functional bacteria in a complex microbial community. *ISME J.* **2015**, *9*, 603–614.
- (16) Wang, X.; Zhao, X.; Li, H.; Jia, J.; Liu, Y.; Ejenavi, O.; Ding, A.; Sun, Y.; Zhang, D. Separating and characterizing functional alkane degraders from crude-oil-contaminated sites via magnetic nanoparticle-mediated isolation. *Res. Microbiol.* **2016**, *167*, 731–744.
- (17) Handelsman, J. Metagenomics: Application of Genomics to Uncultured Microorganisms. *Microbiol. Mol. Biol. Rev.* **2005**, *69*, 195.
- (18) Chen, Y.; Murrell, J. C. When metagenomics meets stable-isotope probing: progress and perspectives. *Trends Microbiol.* **2010**, *18*, 157–163.
- (19) Castañeda, L. E.; Barbosa, O. Metagenomic analysis exploring taxonomic and functional diversity of soil microbial communities in Chilean vineyards and surrounding native forests. *PeerJ* **2017**, *5*, No. e3098.
- (20) Song, Y.; Yin, H.; Huang, W. E. Raman activated cell sorting. *Curr. Opin. Chem. Biol.* **2016**, *33*, 1–8.
- (21) Li, M.; Xu, J.; Romero-Gonzalez, M.; Banwart, S. A.; Huang, W. E. Single cell Raman spectroscopy for cell sorting and imaging. *Curr. Opin. Biotechnol.* **2012**, *23*, 56–63.
- (22) Jing, X.; Gou, H.; Gong, Y.; Su, X.; Xu, L.; Ji, Y.; Song, Y.; Thompson, I. P.; Xu, J.; Huang, W. E. Raman-activated cell sorting and metagenomic sequencing revealing carbon-fixing bacteria in the ocean. *Environ. Microbiol.* **2018**, *20*, 2241–2255.
- (23) Li, H.-Z.; Bi, Q.-f.; Yang, K.; Zheng, B.-X.; Pu, Q.; Cui, L. D2O-Isotope-Labeling Approach to Probing Phosphate-Solubilizing Bacteria in Complex Soil Communities by Single-Cell Raman Spectroscopy. *Anal. Chem.* **2019**, *91*, 2239–2246.
- (24) Berry, D.; Mader, E.; Lee, T. K.; Woebken, D.; Wang, Y.; Zhu, D.; Palatinszky, M.; Schintlmeister, A.; Schmid, M. C.; Hanson, B. T.; Shterzer, N.; Mizrahi, I.; Rauch, I.; Decker, T.; Bocklitz, T.; Popp, J.; Gibson, C. M.; Fowler, P. W.; Huang, W. E.; Wagner, M. Tracking heavy water (D2O) incorporation for identifying and sorting active microbial cells. *Proc. Natl. Acad. Sci. U.S.A.* **2015**, *112*, E194–E203.
- (25) Wang, Y.; Huang, W. E.; Cui, L.; Wagner, M. Single cell stable isotope probing in microbiology using Raman microspectroscopy. *Curr. Opin. Biotechnol.* **2016**, *41*, 34–42.
- (26) Wang, Y.; Xu, J.; Kong, L.; Liu, T.; Yi, L.; Wang, H.; Huang, W. E.; Zheng, C. Raman-deuterium isotope probing to study metabolic activities of single bacterial cells in human intestinal microbiota. *Microb. Biotechnol.* **2020**, *13*, 572–583.
- (27) Cui, L.; Yang, K.; Li, H.-Z.; Zhang, H.; Su, J.-Q.; Paraskevaidi, M.; Martin, F. L.; Ren, B.; Zhu, Y.-G. Functional Single-Cell Approach to Probing Nitrogen-Fixing Bacteria in Soil Communities by Resonance Raman Spectroscopy with ¹⁵N₂ Labeling. *Anal. Chem.* **2018**, *90*, 5082–5089.
- (28) Wang, Y.; Xu, J.; Kong, L.; Li, B.; Li, H.; Huang, W. E.; Zheng, C. Raman-activated sorting of antibiotic-resistant bacteria in human gut microbiota. *Environ. Microbiol.* **2020**, *22*, 2613–2624.
- (29) Li, J.; Luo, C.; Zhang, D.; Song, M.; Cai, X.; Jiang, L.; Zhang, G. Autochthonous Bioaugmentation-Modified Bacterial Diversity of Phenanthrene Degraders in PAH-Contaminated Wastewater as Revealed by DNA-Stable Isotope Probing. *Environ. Sci. Technol.* **2018**, *52*, 2934–2944.
- (30) Edgar, R. C. Search and clustering orders of magnitude faster than BLAST. *Bioinformatics* **2010**, *26*, 2460–2461.
- (31) Werner, J. J.; Koren, O.; Hugenholtz, P.; Desantis, T. Z.; Walters, W. A.; Caporaso, J. G.; Angenent, L. T.; Knight, R.; Ley, R. E. Impact of training sets on classification of high-throughput bacterial 16S rRNA gene surveys. *ISME J.* **2012**, *6*, 94–103.
- (32) Sun, Y.; Yin, M.; Zheng, D.; Wang, T.; Zhao, X.; Luo, C.; Li, J.; Liu, Y.; Xu, S.; Deng, S.; Wang, X.; Zhang, D. Different acetonitrile degraders and degrading genes between anaerobic ammonium oxidation and sequencing batch reactor as revealed by stable isotope probing and magnetic-nanoparticle mediated isolation. *Sci. Total Environ.* **2021**, *758*, 143588.
- (33) Jiang, L.; Luo, C.; Zhang, D.; Song, M.; Mei, W.; Sun, Y.; Zhang, G. Shifts in a Phenanthrene-Degrading Microbial Community are Driven by Carbohydrate Metabolism Selection in a Ryegrass Rhizosphere. *Environ. Sci. Technol.* **2021**, *55*, 962–973.
- (34) Li, J.; Peng, K.; Zhang, D.; Luo, C.; Cai, X.; Wang, Y.; Zhang, G. Autochthonous bioaugmentation with non-direct degraders: A new strategy to enhance wastewater bioremediation performance. *Environ. Int.* **2020**, *136*, 105473.
- (35) Kweon, O.; Kim, S.-J.; Jones, R. C.; Freeman, J. P.; Adjei, M. D.; Edmondson, R. D.; Cerniglia, C. E. A polyomic approach to elucidate the fluoranthene-degradative pathway in *Mycobacterium vanbaalenii* PYR-1. *J. Bacteriol.* **2007**, *189*, 4635–4647.
- (36) Langmead, B.; Trapnell, C.; Pop, M.; Salzberg, S. L. Ultrafast and memory-efficient alignment of short DNA sequences to the human genome. *Genome Biol.* **2009**, *10*, R25.
- (37) Li, D.; Liu, C.-M.; Luo, R.; Sadakane, K.; Lam, T.-W. MEGAHIT: an ultra-fast single-node solution for large and complex metagenomics assembly via succinct de Bruijn graph. *Bioinformatics* **2015**, *31*, 1674–1676.
- (38) Seemann, T. Prokka: rapid prokaryotic genome annotation. *Bioinformatics* **2014**, *30*, 2068–2069.
- (39) Uritskiy, G. V.; DiRuggiero, J.; Taylor, J. MetaWRAP—a flexible pipeline for genome-resolved metagenomic data analysis. *Microbiome* **2018**, *6*, 158.
- (40) Abubucker, S.; Segata, N.; Goll, J.; Schubert, A. M.; Izard, J.; Cantarel, B. L.; Rodriguez-Mueller, B.; Zucker, J.; Thiagarajan, M.; Henrissat, B.; White, O.; Kelley, S. T.; Methé, B.; Schloss, P. D.; Gevers, D.; Mitreva, M.; Huttenhower, C. Metabolic Reconstruction for Metagenomic Data and Its Application to the Human Microbiome. *PLoS Comput. Biol.* **2012**, *8*, No. e1002358.
- (41) Thomas, F.; Corre, E.; Cébron, A. Stable isotope probing and metagenomics highlight the effect of plants on uncultured phenanthrene-degrading bacterial consortium in polluted soil. *ISME J.* **2019**, *13*, 1814–1830.
- (42) Katoh, K.; Kuma, K.-i.; Toh, H.; Miyata, T. MAFFT version 5: improvement in accuracy of multiple sequence alignment. *Nucleic Acids Res.* **2005**, *33*, 511–518.
- (43) Waterhouse, A. M.; Procter, J. B.; Martin, D. M.; Clamp, M.; Barton, G. J. Jalview Version 2—a multiple sequence alignment editor and analysis workbench. *Bioinformatics* **2009**, *25*, 1189–1191.
- (44) Li, J.; Lu, Q.; Liu, T.; Zhou, S.; Yang, G.; Zhao, Y. *Paenibacillus guangzhouensis* sp. nov., an Fe(III)- and humus-reducing bacterium from a forest soil. *Int. J. Syst. Evol. Microbiol.* **2014**, *64*, 3891–3896.

(45) Huang, C.; Zeng, Y.; Luo, X.; Ren, Z.; Lu, Q.; Tian, Y.; Gao, S.; Wang, S.; Harrad, S.; Mai, B. Tracing the sources and microbial degradation of PCBs in field sediments by a multiple-line-of-evidence approach including compound-specific stable isotope analysis. *Water Res.* **2020**, *182*, 115977.

(46) R Core Team R: *A language and environment for statistical computing*, 2011; Vol 1, pp 12–21.

(47) Hu, W.; Liang, J.; Ju, F.; Wang, Q.; Liu, R.; Bai, Y.; Liu, H.; Qu, J. Metagenomics Unravels Differential Microbiome Composition and Metabolic Potential in Rapid Sand Filters Purifying Surface Water Versus Groundwater. *Environ. Sci. Technol.* **2020**, *54*, 5197–5206.

(48) Lewis, W. H.; Tahon, G.; Geesink, P.; Sousa, D. Z.; Ettema, T. J. G. Innovations to culturing the uncultured microbial majority. *Nat. Rev. Microbiol.* **2021**, *19*, 225–240.

(49) Cross, K. L.; Campbell, J. H.; Balachandran, M.; Campbell, A. G.; Cooper, C. J.; Griffen, A.; Heaton, M.; Joshi, S.; Klingeman, D.; Leys, E.; Yang, Z.; Parks, J. M.; Podar, M. Targeted isolation and cultivation of uncultivated bacteria by reverse genomics. *Nat. Biotechnol.* **2019**, *37*, 1314–1321.

(50) Mei, W.; Sun, H.; Song, M. K.; Jiang, L. F.; Li, Y. T.; Lu, W. S.; Ying, G. G.; Luo, C. L.; Zhang, G. Per- and polyfluoroalkyl substances (PFASs) in the soil-plant system: Sorption, root uptake, and translocation. *Environ. Int.* **2021**, *156*, 106642.

(51) Haider, S.; Wagner, M.; Schmid, M. C.; Sixt, B. S.; Christian, J. G.; Häcker, G.; Pichler, P.; Mechtler, K.; Müller, A.; Baranyi, C.; Toenshoff, E. R.; Montanaro, J.; Horn, M. Raman microspectroscopy reveals long-term extracellular activity of chlamydiae. *Mol. Microbiol.* **2010**, *77*, 687–700.

(52) Martín, H. G.; Ivanova, N.; Kunin, V.; Warnecke, F.; Barry, K. W.; McHardy, A. C.; Yeates, C.; He, S.; Salamov, A. A.; Szeto, E.; Dalin, E.; Putnam, N. H.; Shapiro, H. J.; Pangilinan, J. L.; Rigoutsos, I.; Kyripides, N. C.; Blackall, L. L.; McMahon, K. D.; Hugenholtz, P. Metagenomic analysis of two enhanced biological phosphorus removal (EBPR) sludge communities. *Nat. Biotechnol.* **2006**, *24*, 1263–1269.

(53) Langmead, B.; Trapnell, C.; Pop, M.; Salzberg, S. L. Ultrafast and memory-efficient alignment of short DNA sequences to the human genome. *Genome Biol.* **2009**, *10*, R25.

(54) Carini, P. A “Cultural” Renaissance: Genomics Breathes New Life into an Old Craft. *mSystems* **2019**, *4*, No. e00092-19.

(55) Liu, Z.-P.; Wang, B.-J.; Liu, Y.-H.; Liu, S.-J. *Novosphingobium taihuense* sp. nov., a novel aromatic-compound-degrading bacterium isolated from Taihu Lake, China. *Int. J. Syst. Evol. Microbiol.* **2005**, *55*, 1229–1232.

(56) Zhang, J.; Liu, Y.-X.; Guo, X. X.; Qin, Y.; Garrido-Oter, R.; Schulze-Lefert, P.; Bai, Y. High-throughput cultivation and identification of bacteria from the plant root microbiota. *Nat. Protoc.* **2021**, *16*, 988.

(57) Zhaxybayeva, O.; Lapierre, P.; Gogarten, J. P. Genome mosaicism and organismal lineages. *Trends Genet.* **2004**, *20*, 254–260.

(58) Huerta-Cepas, J.; Szklarczyk, D.; Heller, D.; Hernández-Plaza, A.; Forslund, S. K.; Cook, H.; Mende, D. R.; Letunic, I.; Rattei, T.; Jensen, L. J.; von Mering, C.; Bork, P. eggNOG 5.0: a hierarchical, functionally and phylogenetically annotated orthology resource based on 5090 organisms and 2502 viruses. *Nucleic Acids Res.* **2019**, *47*, D309–D314.

(59) Liu, C.; Cui, Y.; Li, X.; Yao, M. microeco: an R package for data mining in microbial community ecology. *FEMS Microbiol. Ecol.* **2021**, *97*, fiae255.

Recommended by ACS

Macroporous Silicone Chips for Decoding Microbial Dark Matter in Environmental Microbiomes

Ahmed E. Zoheir, Christof M. Niemeyer, *et al.*

OCTOBER 26, 2022
ACS APPLIED MATERIALS & INTERFACES

READ 

Phenotypic Differentiation of Autotrophic and Heterotrophic Bacterial Cells Using Raman-D₂O Labeling

Georgette Azemtsop Matanfack, Jürgen Popp, *et al.*

MAY 24, 2022
ANALYTICAL CHEMISTRY

READ 

Deciphering Black Extrinsic Tooth Stain Composition in Children Using Metaproteomics

Christophe Hirtz, Jerome Vialaret, *et al.*

FEBRUARY 25, 2022
ACS OMEGA

READ 

Why Environmental Biomarkers Work: Transcriptome–Proteome Correlations and Modeling of Multistressor Experiments in the Marine Bacterium *Tric...*

Nathan G. Walworth, Eric A. Webb, *et al.*

DECEMBER 02, 2021
JOURNAL OF PROTEOME RESEARCH

READ 

Get More Suggestions >